OXFORD

Food Quality and Safety, 2020, 4, 181–192
doi:10.1093/fqsafe/fyaa025
Article
Advance Access publication 11 September 2020

Article

Application of electronic nose and GC–MS for detection of strawberries with vibrational damage

Jingshan Rao, *,† Yuchen Zhang,*,† Zhichao Yang,* Shaojia Li,* Di Wu,*,, Chongde Sun*, and Kunsong Chen***

*College of Agriculture and Biotechnology/Zhejiang Provincial Key Laboratory of Horticultural Plant Integrative Biology/The State Agriculture Ministry Laboratory of Horticultural Plant Growth, Development and Quality Improvement, Zhejiang University, Hangzhou, China and **Zhejiang University Zhongyuan Institute, Zhengzhou, China

†Jingshan Rao and Yuchen Zhang contributed equally to this work.

Correspondence to: Di Wu, College of Agriculture and Biotechnology/Zhejiang Provincial Key Laboratory of Horticultural Plant Integrative Biology/The State Agriculture Ministry Laboratory of Horticultural Plant Growth, Development and Quality Improvement, Zhejiang University, Zijingang Campus, Hangzhou 310058, China. E-mail: di_wu@zju.edu.cn

Received 17 August 2020; Revised 8 September 2020; Editorial decision 9 September 2020.

Abstract

Objectives: This study evaluated the potential of using electronic nose (e-nose) technology to non-destructively detect strawberry fruits with vibrational damage based on their volatile substances (VOCs).

Materials and methods: Four groups of strawberries with different durations of vibrations (0, 0.5, 1, and 2 h) were prepared, and their e-nose signals were collected at 0, 1, 2, and 3 days after vibration treatment.

Results: The results showed that when the samples from all four sampling days during storage were used for modelling, both the levels of vibrational damage and the day after the damage happened were accurately predicted. The best models had residual prediction deviation values of 2.984 and 5.478. The discrimination models for damaged strawberries also obtained good classification results, with an average correct answer rate of calibration and prediction of 99.24%. When the samples from each sampling day or vibration time were used for modelling, better results were obtained, but these models were not suitable for an actual situation. The gas chromatography–mass spectrophotometry results showed that the VOCs of the strawberries varied after experiencing vibrations, which was the basis for e-nose detection.

Limitations: The changes in VOCs released by other forces should be studied in the future.

Conclusions: The above results showed the potential use of e-nose technology to detect strawberries that have suffered vibrational damage.

Graphical Abstract

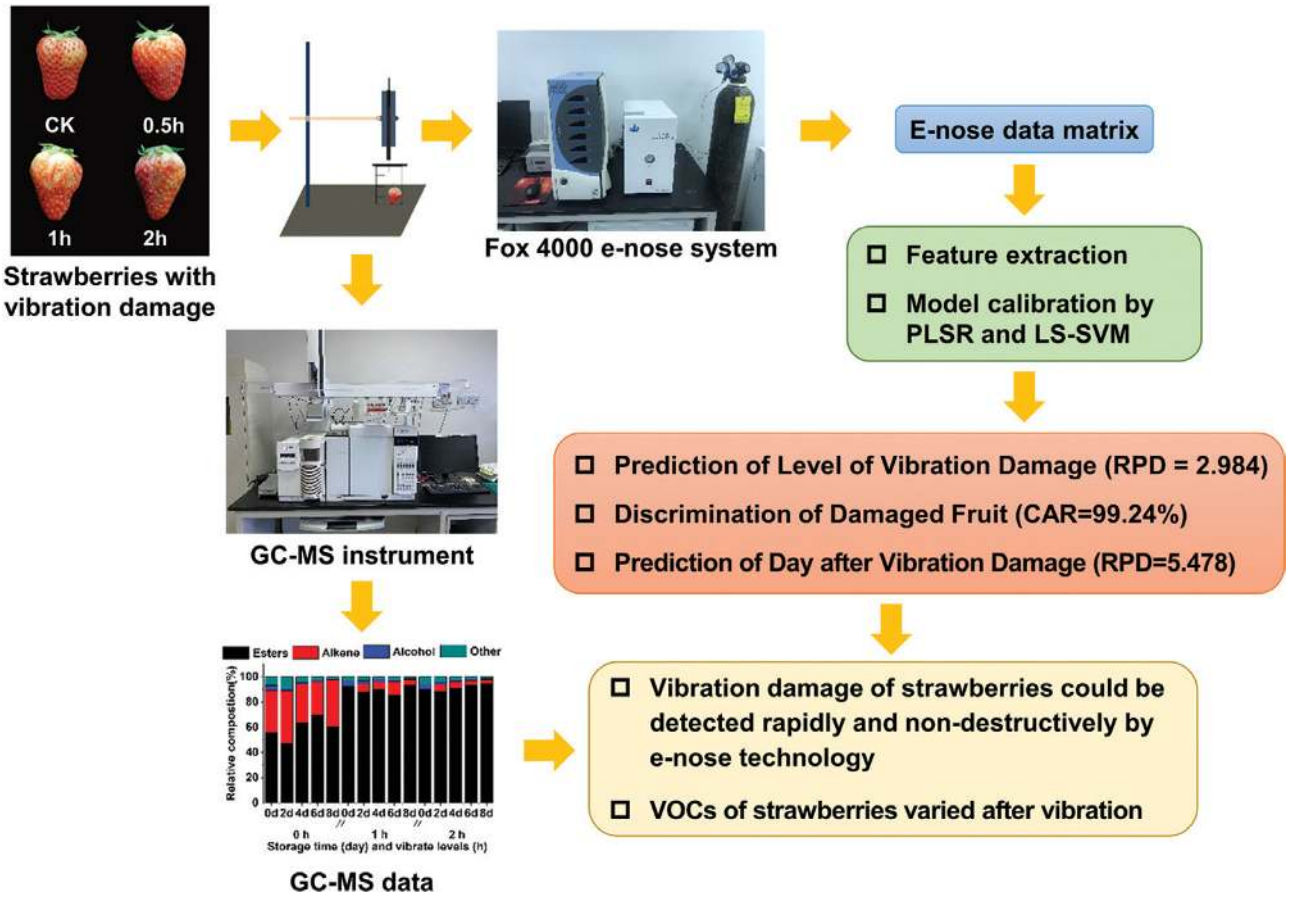

Key words: strawberry; electronic nose; vibrational damage; non-destructive; GC–MS.

Introduction

Strawberries (*Fragaria* × *ananassa Duch*) are members of the rose family and are cultivated worldwide. This fruit is widely appreciated for its pleasant aroma, colour, and taste; it is also a low-calorie and low-sugar fruit. Moreover, strawberries are rich in many substances, such as vitamin C, folates, carotene, anthocyanin, and minerals, among which vitamins and polyphenols have antioxidant and anti-inflammatory effects, giving the fruit a large market and great commercial value (Aaby *et al.*, 2005; Giampieri *et al.*, 2012). Strawberries are consumed popularly as jam, ice cream, pies, and milkshakes. Artificial strawberry flavourings and aromas are often used in the production of cakes, lip glosses, cosmetics, and soaps, and fresh strawberries are also widely enjoyed by consumers.

Due to their soft texture, many fruits can easily become mechanically damaged in their supply chains (Li ZG *et al.*, 2013). Physiological deterioration will occur after such damage. After being damaged by squeezing and vibrations, tomatoes had lower firmness, greater PME activity, and juice consistency (Aaby *et al.*, 2005). Held *et al.* (2015) found that after 60 days of storage, mechanically damaged Yali pears had a 20.7% higher water loss rate and a 4.2% lower firmness than normal pears, with a significantly reduce acid-sugar ratio. Cosmetic defects in fruits can also be attributed to mechanical damage. As a critical determinant of fruit quality, appearance can significantly influence a consumer's desire to purchase (Kader, 2002) and affect the potential possibility of repeated purchases (Jaeger *et al.*, 2016). Strawberries are especially delicate, are susceptible to squeezing and vibration, and have a high respiration rate, which makes strawberries difficult to store and causes heavy economic losses (Liu *et al.*, 2018; Nguyen *et al.*, 2020).

In the postharvest supply chains, such as in cold storage rooms or on trucks, the rapid freshness evaluation and mechanical damage detection of fruit are important for the early determination of fruit quality deterioration, which closely relates to subsequent freshness preservation and retail strategies. Currently, the detection of mechanical damage to fruit is mainly carried out by measuring the sizes and shapes of bruises, such as the bruise area, bruise volume, bruise number, bruise diameter, bruise depth, bruise proportion, and bruise index (Li and Thomas, 2014). Nevertheless, such measurements are time-consuming, and labour-intensive, and some of them are destructive. Moreover, these measurements involve selective inspection. This means that only a few samples will be measured. In practical industrial applications, participants in all links of the supply chain, such as growers, distributors, sellers, and customers, are accustomed to observing the decay and damage of fruits directly with the naked eye, but with inevitable deficiencies such as being

subjective, time-consuming, and boring. Therefore, it is necessary to find a detection technology that can quickly determine the quality deterioration of postharvest fruits in their supply chains, to provide information to ensure prompt changes in transportation, storage, and retail decisions. This is an important step for realizing the intelligent control of postharvest fruit supply chains, thereby ensuring fruit quality, reducing fruit losses, and improving efficiency.

Because they are rapid and non-destructive, spectroscopy or imaging technologies, such as computer vision, visible and near-infrared spectroscopy, and hyperspectral imaging techniques, are often used for the detection of fruit freshness and mechanical damage (Wu and Sun, 2013a, 2013b, 2013c). Nevertheless, in their supply chains, fruits are commonly packaged in containers made of corrugated fibreboard or plastic, covered by inner packaging materials, and are then placed in dark environments, such as cold storage or carriage without light sources, which all make it difficult to judge whether postharvest fruits were damaged through spectroscopy or imaging inspection in their supply chains. Consequently, we need a technique that can remain effective for the detection of damaged fruits even when the fruits are packaged in the dark.

Volatile substances (VOCs) are key indexes in fruit quality assessment and important considerations for customers. There are various kinds of VOCs in fruit, including aldehydes, esters, lactones, and terpenes. These VOC substances are closely related to many factors, such as fruit cultivation conditions, harvest maturity, and postharvest environment. Although VOCs only occupy 0.001–0.01% of strawberries by weight, VOCs are significant components that determine the flavour of strawberries (Larsen and Poll, 1992). More than 360 kinds of VOCs are found in fresh strawberries, including esters, alcohols, ketones, furans, terpenes, aldehydes, and sulfur compounds (Zabetakis and Holden, 1997). Of all the compounds above, esters are the richest and the main source of the fruit and flower fragrances of strawberries, accounting for 10 of the 15 most common VOCs in strawberries (Jetti *et al.*, 2007). Cultivars, cultivation conditions, mechanical damage, storage time, and pathogenic fungal disease also effect the VOCs of strawberries (Hamiltonkemp *et al.*, 2003; Pan *et al.*, 2014; Xing *et al.*, 2018; Parrapalma *et al.*, 2019). As there is a correlation between VOCs and the quality deterioration of the fruit, VOCs could be an indicator to determine whether the fruit has been mechanically damaged.

The electronic nose (e-nose) is a widely used bionic olfactory system with high efficiency and simplicity. This system can imitate human olfactory sensors for online and non-destructive odour recognition. An e-nose instrument consists of a sampling system, a signal processing system, and the core part, a gas sensor array, which is decisive to the system's sensitivity and accuracy. There are many kinds of gas sensors, including conductivity sensors, piezoelectric sensors, field-effect sensors, optical fibre sensors, and metal sensors, which are most popular for their low cost and high sensitivity (Srivastava and Sadistap, 2018). E-nose has been used to classify fruit grades and predict fruit quality. Centonze *et al.* (2019) used an e-nose instrument to classify oranges with three different geographical origins and found that the combination of the stepwise decorrelation of the variables and linear discriminant analysis (SELECT/LDA) offered the best accuracy. Liu *et al.* (2018) discriminated peaches with pathogenic fungi contamination using an e-nose, and colony counts were predicted with a residual prediction deviation (RPD) of 2.80–4.16. Xing *et al.* (2018) developed a portable e-nose system for strawberry quality classification, achieving higher accuracy (96.9%) than a commercial e-nose system (94.4%), though the former's cost was nearly 30-fold lower than that of the latter. In our previous research, e-nose technology was used to measure the VOCs in peaches and to determine whether the fruit was decayed, obtaining a *correct answer rate (CAR)* of prediction of 95.83% (Wei *et al.*, 2018). In another study, we used e-nose technology and near-infrared spectroscopy to predict the number of days left before the decay of peach fruit; the best prediction model had a CAR of 82.26% (Huang *et al.*, 2017a). To the best of our knowledge, e-nose technology has not been used to detect strawberries with mechanical damage. Moreover, in previous studies, the collection of e-nose signals from fruit with mechanical damage was mainly conducted shortly after the fruit was damaged. Moreover, these studies did not consider a situation in which the quality of the fruit continues to deteriorate, resulting in its appearance and VOC content changing. Indeed, the VOCs of a damaged fruit are usually different at different times after the fruit is damaged. It is also difficult to determine when fruit became damaged and collect the e-nose signal immediately after that damage in practical applications. Therefore, for the study of fruit mechanical damage detection and to make the established model more suitable for actual situations, it is necessary to collect e-nose data at different times after the fruit is mechanically damaged.

The objective of this work is to evaluate the potential of using e-nose technology to non-destructively detect vibrational damage in strawberries. The specifically established chemometric models include one for predicting the levels of vibrational damage, one for distinguishing the damaged fruit, and one for predicting the day after the damage happened. Moreover, the variational patterns of VOCs due to the vibrational damage of strawberries were characterized by a gas chromatography–mass spectrophotometry (GC–MS) analysis. Notably, in the actual supply chain process, the detection of volatile substances in fruits should be non-destructive; otherwise, the tested fruit cannot be sold later. Therefore, in this work, the acquisition of the VOCs of the damaged strawberries for both the GC-MS measurements and e-nose detection was based on examining the whole fruit in a non-destructive way. In addition, a GC–MS measurement was also carried out on the ground fruit flesh to further analyse the variation of VOCs in the damaged fruits.

Materials and Methods

Sample preparation

Hongyan strawberries (*Fragaria* × *ananassa Duch*) were harvested at commercial maturity from an orchard in Hangzhou, Zhejiang province, P.R. China, in March, 2018, and were transported to a laboratory in Hangzhou, Zhejiang province, P.R. China, on the same day. In the experiment, 264 strawberries that were uniform in size and without mechanical damage were selected. The strawberries were divided into four groups with different durations of vibrations to simulate different transport distances—namely, a group of strawberries without vibrations (0 h, Group I), a group of strawberries placed under vibrations for 0.5 h (Group II), a group of strawberries placed under vibrations for 1 h (Group III), and a group of strawberries placed under vibrations for 2 h (Group IV). A TH-600 vibration test system (Suzhou Sushi Testing Instrument Co., Ltd., Suzhou, China) was used, and the vibration frequency was set to ASTM D4728 Section 6 (ASTM, 2016), which is the standard for the random vibration detection of transport containers and can simulate mechanical damage during transportation. After corresponding treatments, all groups of strawberries were placed into a cold room for further storage. The environment for both the vibration test and storage was maintained at a temperature of 15 °C and humidity of 90–95%. The e-nose signals were collected at 0 days (right after vibration treatment), 1, 2, and 3 days after the vibration treatment. At each sampling day, the e-nose signals for 30 strawberries were measured in each group.

E-nose instrument and data acquisition

A Fox 4000 e-nose system (Alpha MOS, Toulouse, France) was used for e-nose acquisition. This system consists of three parts: a gas sampling system, a sensor chamber, and data analysis software. The sensor chamber is divided into three chambers (T chamber, P chamber and LY chamber), and all chambers contain six metal oxide gas sensors (MOS), each of which is a round or flat ceramic substrate coated with a metal oxide semiconductor film (mainly zinc oxide, tin dioxide, and titanium dioxide, or iron (III) oxide). Before data measurement, the MOS sensor was calibrated with standard samples (n-propanol, acetone, and isopropanol) to ensure its stability. To ensure the accuracy of the collected data, after each measurement, the sensors were cleaned with dry and purified air processed by an air generator with a $CaCl_2$ dehydration column.

Before e-nose acquisition, the single whole fruit was placed into a 100 ml clean beaker, which was sealed with parafilm and left to stand for 30 min to give enough time for the VOCs in the headspace to reach a dynamic balance. After sealing, a 2.5 ml syringe was used to puncture the parafilm and repeatedly pump and inject the gas 4–5 times to disperse the VOCs evenly. After that, 2 ml of the gas was pumped out of the beaker and injected into the injection port of the e-nose system. Then, the gas was pumped into the sensor chamber at a consonant rate of 150 ml·min^{-1}. The detection time was 120 s, and the cleaning time was 240 s. A figure of the sensors signals in e-nose for one typical sample is shown in Figure 1.

Multivariate data analysis

The measured e-nose signal (0 to 120 s) was exported from the control software for model calibration (Xin *et al.*, 2018). The complete data (ENAll) collected in these two minutes contained over 2000 variables. Some of these variables could contain redundant noise signals, which would increase the modelling time and reduce the accuracy of the model. Extracting the features of the e-nose data and searching for valuable data for calculations can simplify the model prediction process. In this study, a total of eleven features were extracted: 1. the data of the response curve at the 10th, 20th, 40th, 60th, 80th, 100th, and 120th s, named EN10, EN20, EN40, EN60, EN80, EN100, and EN120, respectively; 2. the area between the response curve and the X-axis (ENSUM); 3. the maximum value of the response curve (ENMax); 4. the minimum value of the response curve (ENMin); and 5. the difference between the maximum and minimum values of the response curve (ENDiff).

Two algorithms were used for model calibration: partial least squares regression (PLSR) and least squares support vector machine (LS-SVM). PLSR is a multivariate statistical linear regression method that is widely used to establish reliable regression models (Huang *et al.*, 2017b; Chen *et al.*, 2020). The min principle of PLSR is to extract the orthogonal factors of latent variables (LVs) and establish the regression relationship between the data set and the corresponding reference value. LVs are obtained by simultaneously decomposing the e-nose data (dependent variable) and the damage levels or storage time (independent variable), as in this work. Therefore, PLSR can be regarded as a hybrid calculation of PCA, canonical correlation analysis (CCA), and multiple linear regression, thus combining all their advantages. LS-SVM is a classic nonlinear regression method suitable for the calculation of small sample data (Huang *et al.*, 2015; Wei *et al.*, 2018). It commonly uses a radial basis function (RBF) kernel to map the input features into a high-dimensional feature space, thereby transforming linear inseparable problems into constrained quadratic programming problems (Li *et al.*, 2007). A grid-search technique with leave-one-out cross-validation was used to obtain the optimal values of the regularization parameter γ and the RBF kernel function parameter σ^2 in the LS-SVM model. In addition, the samples for calibration and prediction were selected by a sample set partitioning based on the joint X-Y distance (SPXY) algorithm (Galvao *et al.*, 2005).

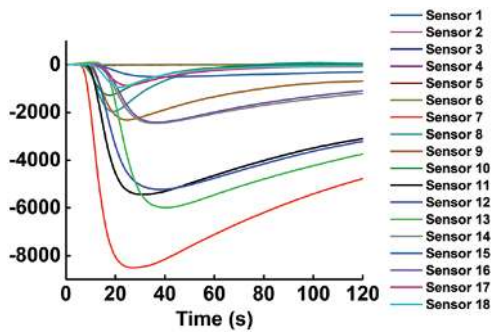

Figure 1. Sensors signals in electronic nose (e-nose) for one typical sample.

The performance of the models in predicting the level of vibrational damage and the day after the damaged happened was evaluated by the root-mean-square error of calibration (RMSEC) and the correlation coefficient of calibration (Rc) during the calibration process and the root-mean-square error of prediction (RMSEP), the correlation coefficient of prediction (Rp), and RPD during the prediction process. In addition, the absolute difference between RMSEC and RMSEP (AB_RMSE) was used to evaluate the robustness of the established regression model. The smaller the AB_RMSE value, the better the robustness of the model. A good model should have higher Rc, Rp, and RPD values and lower RMSEC, RMSEP, and AB_RMSE values. The performance of the models in distinguishing the damaged fruit was evaluated by their CAR. The correct answer rate is the ratio of the number of correctly classified samples to the number of all samples.

GC–MS measurement

7860N-5973-C (Agilent, Wilmington, USA) was used for the GC-MS measurement, which was carried out at 2, 4, 6, and 8 d after vibrations. Two sampling methods were adopted in the GC–MS measurements. One was based on non-destructive sampling, which measured the VOCs in the headspace of intact strawberries without grinding the sample. The other was based on destructive sampling, which measured the VOCs of the ground fruit flesh. At each sampling day, three strawberries were used for non-destructive GC–MS measurements and nine strawberries were ground for destructive GC–MS measurement.

The non-destructive GC-MS measurement used manual injection. A single whole strawberry was placed in a 100 ml beaker and sealed with parafilm for 30 min. A fibre (PDMS/DVB, 65 µm, capillary column, USA) was used for the Headspace Solid Phase Micro-Extraction (HS-SPME) for 30 min and was then inserted into the inlet and desorbed at a temperature of 240 °C for 5 min for the GC–MS measurement. The main parameters for gas chromatography included high-purity helium as the carrier gas at a flow rate of 1.0 ml/min and a DB-WAX quartz capillary column (30 m, 0.25 mm, 0.25 µm) as the column model, whose temperature was initially 40 °C and then increased to 100 °C at a rate of 3 °C/min; the temperature then kept increasing up to 245 °C at a rate of 5 °C/min. The parameters of the mass spectrometer were an electron impact ion source (EI ion source) ionized at an electron energy of 70 eV, with a transition temperature of 250 °C and an ion source temperature of 230 °C.

The destructive GC–MS measurement used automatic injection. The strawberries were chopped and frozen in liquid nitrogen and then ground into powder under low temperature. Each group of strawberry samples contained three experimental replicates and three biological replicates. Strawberry powder (5 g) was placed in a 20 ml special headspace bottle supplemented with 5 ml of saturated calcium chloride solution (Prat *et al.*, 2014) and 20 µL of 2-octanone at a concentration of 0.8 mg/ml (Li L *et al.*, 2013) as an internal standard. After being shaken evenly, the bottle was placed in the automatic sample tray and pierced by the extraction fibre with a depth of 40 mm for 30 min for SPME at 45 °C. Then, the fibre was inserted into the inlet and desorbed for 5 min under a temperature of 240 °C. The parameters for the destructive GC–MS measurement were as same as those for the non-destructive GC–MS measurement.

Results

Detection of levels of vibrational damage

To evaluate whether e-nose technology can be used to detect the level of vibrational damage suffered by strawberry fruits, prediction models were established based on the full e-nose variables called ENAll and the extracted eleven features. The durations of vibrations were used as the reference data of the levels of vibrational damage. Table 1 shows the results of the detected levels of vibrational damage based on strawberries under all storage times (360 samples were used for calibration and the remaining 120 samples for prediction). The average Rc and Rp were used as the standard to evaluate the established models. The PLSR-ENAll model was shown to be the best PLSR model, whereas the PLSR-ENMax model was the best PLSR model based on the extracted features. However, in comparison, the results of the LS-SVM models were significantly better than those of the PLSR models, except for the LS-SVM-ENDiff model. The average Rc and Rp for all LS-SVM models (except the LS-SVM-ENDiff model) was 0.951, whereas that of all the PLSR models was only 0.589. Although the AB_RMSE values of the LS-SVM models were generally higher than those of the PLSR models, they were still in an acceptable range. According to RPD and AB_RMSE, the best model for predicting the level of vibrational damage was the LS-SVM-ENAll model. Nevertheless, this model showed overfitting. Therefore, the LS-SVM-ENSum model was considered to be the best. The above results show that e-nose technology can be used to detect the level of vibrational damage, while the LS-SVM algorithm was more suitable for analysing e-nose data than PLSR in this case.

Besides the samples under all storage times used for modelling (Table 1), models were also established based only on samples whose e-nose signals were collected at 0 days (right after vibration treatment), 1, 2, or 3 days after vibration treatment, and their results are shown in Table 2. On each sampling day, 90 samples were used for the calibration and another 30 samples for the prediction, and only the results for the ENAll model and the best model based on the extracted variables are given. Based on the samples just after the vibration (0 days), the prediction accuracy of the four models was similar, where the RMSEC and RMSEP values were both below 0.3, and their AB_RMSE values were also lower than 1. For the samples only one day after the end of the vibrations, the accuracy of the models was generally better than that for the samples at 0 days. Based on samples taken 2 days after the end of the vibrations, the results of the four models were better than those of other days, and the RPDs were all above 4.5. For the samples on the third day after vibrations, the PLSR models were slightly worse than those for the samples on the second day, whereas the accuracy of the LS-SVM models was about the same. In general, when considering samples with different days of storage, ENAll-based models and the models established based on feature variables can accurately predict the

Table 1. Detected levels of vibrational damage based on strawberries under all storage times.

Feature variables	Calibration method	Calibration			Prediction				AB_RMSE
		R_c	Rc^2	RMSEC	R_p	Rp^2	RMSEP	RPD	
ENAll	PLSR	0.686	0.471	0.824	0.655	0.394	0.836	1.290	0.012
ENMax	PLSR	0.616	0.379	0.893	0.709	0.432	0.809	1.342	0.083
ENMin	PLSR	0.602	0.362	0.905	0.593	0.319	0.886	1.213	0.019
EN_{Sum}	PLSR	0.593	0.352	0.912	0.604	0.339	0.873	1.235	0.039
ENDiff	PLSR	0.455	0.207	1.008	0.445	0.154	0.987	1.096	0.021
EN_{10}	PLSR	0.604	0.365	0.902	0.630	0.333	0.877	1.233	0.026
EN_{20}	PLSR	0.590	0.349	0.914	0.595	0.322	0.884	1.223	0.030
EN_{40}	PLSR	0.545	0.298	0.949	0.575	0.296	0.901	1.197	0.048
EN_{60}	PLSR	0.577	0.333	0.925	0.555	0.290	0.905	1.190	0.020
EN_{80}	PLSR	0.590	0.349	0.914	0.579	0.313	0.890	1.209	0.024
EN_{100}	PLSR	0.592	0.350	0.913	0.556	0.299	0.899	1.197	0.014
EN_{120}	PLSR	0.594	0.353	0.911	0.590	0.331	0.878	1.223	0.033
ENAll	LS-SVM	0.998	0.996	0.073	0.955	0.910	0.321	3.363	0.249
ENMax	LS-SVM	0.980	0.959	0.228	0.935	0.872	0.384	2.804	0.156
ENMin	LS-SVM	0.975	0.948	0.259	0.924	0.853	0.411	2.611	0.152
EN_{Sum}	LS-SVM	0.973	0.945	0.266	0.942	0.881	0.370	2.984	0.104
ENDiff	LS-SVM	0.441	0.102	1.073	0.000	0.000	1.131	0.965	0.057
EN_{10}	LS-SVM	0.979	0.955	0.240	0.886	0.781	0.502	2.147	0.262
EN_{20}	LS-SVM	0.986	0.970	0.198	0.921	0.844	0.424	2.535	0.226
EN_{40}	LS-SVM	0.965	0.927	0.305	0.919	0.842	0.427	2.518	0.121
EN_{60}	LS-SVM	0.978	0.954	0.242	0.931	0.855	0.409	2.717	0.167
EN_{80}	LS-SVM	0.971	0.941	0.275	0.900	0.806	0.473	2.294	0.198
EN_{100}	LS-SVM	0.982	0.963	0.218	0.918	0.840	0.430	2.524	0.212
EN_{120}	LS-SVM	0.974	0.945	0.265	0.923	0.847	0.419	2.567	0.154

LS-SVM, least squares support vector machine; PLSR, partial least squares regression; R_c, correlation coefficient of calibration; RMSEC, root-mean-square error of calibration; RMSEP, root-mean-square error of prediction; R_p, correlation coefficient of prediction. AB_RMSE: the absolute difference between RMSEC and RMSEP.

Table 2. Detection of levels of vibrational damage based on strawberries with different storage times

Time	Feature variables	Calibration method	Calibration			Prediction				AB_RMSE
			R_c	Rc^2	RMSEC	R_p	Rp^2	RMSEP	RPD	
0 d	ENAll	PLSR	0.974	0.949	0.260	0.956	0.908	0.285	3.328	0.025
0 d	EN_{Sum}	PLSR	0.974	0.948	0.264	0.955	0.905	0.290	3.302	0.026
1 d	ENAll	PLSR	0.959	0.919	0.320	0.974	0.929	0.266	3.995	0.054
1 d	ENMin	PLSR	0.964	0.930	0.298	0.961	0.916	0.289	3.566	0.009
2 d	ENAll	PLSR	0.973	0.947	0.253	0.977	0.946	0.251	4.654	0.002
2 d	EN_{Sum}	PLSR	0.972	0.944	0.260	0.976	0.945	0.253	4.590	0.007
3 d	ENAll	PLSR	0.978	0.957	0.236	0.967	0.928	0.289	3.890	0.053
3 d	EN_{Sum}	PLSR	0.973	0.946	0.263	0.972	0.937	0.271	4.016	0.007
0 d	ENAll	LS-SVM	0.982	0.964	0.219	0.962	0.912	0.280	3.388	0.061
0 d	EN_{80}	LS-SVM	0.990	0.980	0.165	0.962	0.923	0.261	3.648	0.096
1 d	ENAll	LS-SVM	0.970	0.941	0.273	0.961	0.908	0.304	3.570	0.030
1 d	ENMax	LS-SVM	0.990	0.981	0.157	0.961	0.907	0.304	3.632	0.148
2 d	ENAll	LS-SVM	0.997	0.994	0.087	0.981	0.959	0.217	5.112	0.130
2 d	EN_{60}	LS-SVM	0.996	0.992	0.101	0.978	0.953	0.235	4.717	0.134
3 d	ENAll	LS-SVM	0.990	0.980	0.162	0.983	0.962	0.208	5.448	0.046
3 d	ENMax	LS-SVM	0.990	0.980	0.162	0.965	0.927	0.291	3.726	0.129

LS-SVM, least squares support vector machine; PLSR, partial least squares regression; R_c, correlation coefficient of calibration; RMSEC, root-mean-square error of calibration; RMSEP, root-mean-square error of prediction; RPD, residual prediction deviation; R_p, correlation coefficient of prediction. AB_RMSE: the absolute difference between RMSEC and RMSEP.

vibration levels of strawberry fruits. In the early storage period after vibration, the results of the PLSR and LS-SVM models were not very different. However, in the later stages of storage, the LS-SVM models were better than the PLSR models. For comparison, the accuracy of the models in Table 2 is generally higher than the accuracy of those in Table 1. In Table 2, the average RPD values of the PLSR and LS-SVM models (all being the best models) are 3.918 and 4.155, respectively, whereas the RPD values of the best PLSR and LS-SVM models in Table 1 are 1.290 and 2.984, respectively. As the models in Table 2 are calibrated based on the samples whose e-nose data were measured at different days after damage, whereas the models in Table 1 are calibrated based on the samples whose e-nose data were measured at all four sampling days, this means that the models calibrated at different days after damage predicted vibrational damage more accurately than those based on all days. Our previous research also found that when the e-nose signals measured at different times after damage were used for modelling at the same time, the prediction accuracy of the model will be lower than that of the models based on the signal measured at each time point (Yang *et al.*, 2020). This might occur because after the fruit suffers mechanical damage, its VOCs change over time; meanwhile, the release of VOCs in the fruit is related to the level of mechanical damage that the fruit suffered. In other words, the quality of damaged strawberries continues to deteriorate, so that the VOCs in the fruits with less vibrational damage in the late storage period could be similar to the VOCs in the fruits with greater vibrational damage in the early storage period. Therefore, when the calibration was based on the samples at all sampling days, the VOCs of the fruits at different times after vibration could have interfered with the model calibration, making the performance of the models generally poorer than that of the models established based on the samples at each sampling day, especially for the PLSR algorithm. Nevertheless, the detection accuracy of the samples from all days, when based on the LS-SVM algorithm, was still satisfactory in the current study. Moreover, from the perspective of industrial applications, samples from different times after vibration should be considered when modelling, rather than just collecting e-nose signals from fruits that recently suffered mechanical damage.

Discrimination of strawberries with or without vibrational damage

In practical applications, sometimes it is not necessary to know the damage level but only to judge whether or not the strawberries are mechanically damaged. Therefore, models were established to classify the strawberries based on the samples from days 0, 1, 2, and 3 and from all 4 days (Table 3). For days 0, 1, 2, and 3, 90 samples were used for the calibration and another 30 samples for the prediction. For all four days, 360 samples were used for the calibration and another 120 samples for the prediction. Compared to other e-nose features, the results of ENDiff were significantly worse. Therefore, the results of the ENDiff models were excluded in the subsequent analysis. When samples from all days were used for modelling, the average CAR of both the calibration and prediction of all PLSR models was 84.99%, whereas that of all LS-SVM models was 96.92%. The best PLSR model was the PLSR-ENAll model, whose average CAR of calibration and prediction was 87.61%; meanwhile, the LS-SVM-ENMin and LS-SVM-EN120 models were the best LS-SVM models, with an average CAR of calibration and prediction of 99.24%. Therefore, when samples from different storage times after vibration were considered, LS-SVM was suggested to be used for model calibration. On the other hand, when samples from different days were considered for modelling separately, there was little difference between the PLSR models and the LS-SVM models. The above results are similar to those for detecting the levels of vibrational damage. In addition, for the samples on days 0, 1, and 2, some models had a CAR of both calibration and prediction that reached 100%, but for the samples on day 3, there was no such model.

Prediction of time after vibrational damage

Predicting when vibrational damage occurs is important for identifying the cause of the damage and optimizing the supply chain. Based on the five sample sets (namely, the three sample sets of fruits vibrated for 0.5, 1, and 2 h, the fruit set without damage (0 h), and the combined sample set), the prediction models for the occurrence time of vibrational damage (0, 1, 2, and 3 d) were established by both the PLSR and LS-SVM algorithms. The reference data were the

Table 3. Discrimination results of strawberries with or without vibrational damage

Feature variables	Calibration Method	0 d		1 d		2 d		3 d		all	
		Calibration	Prediction	Calibration	Prediction	Calibration	Prediction	Calibration	Prediction	Calibration	Prediction
ENAll	PLSR	100.00%	100.00%	90.00%	89.16%	100.00%	100.00%	90.91%	94.12%	85.15%	90.08%
ENMax	PLSR	100.00%	100.00%	90.00%	89.16%	100.00%	98.85%	93.94%	87.06%	80.91%	90.08%
ENMin	PLSR	100.00%	100.00%	93.33%	90.36%	93.33%	96.55%	72.73%	78.82%	79.09%	87.79%
EN_{Sum}	PLSR	100.00%	98.80%	90.00%	89.16%	100.00%	100.00%	90.91%	94.12%	80.91%	89.31%
ENDiff	PLSR	60.00%	78.31%	73.33%	80.72%	90.00%	86.21%	72.73%	63.53%	73.64%	86.26%
EN_{10}	PLSR	100.00%	97.59%	90.00%	90.36%	96.67%	98.85%	96.97%	90.59%	83.64%	88.55%
EN_{20}	PLSR	100.00%	98.80%	83.33%	92.77%	83.33%	95.40%	81.82%	82.35%	79.39%	89.31%
EN_{40}	PLSR	100.00%	95.18%	93.33%	92.77%	96.67%	100.00%	96.97%	89.41%	80.91%	90.08%
EN_{60}	PLSR	100.00%	96.39%	93.33%	90.36%	100.00%	100.00%	90.91%	85.88%	77.88%	87.79%
EN_{80}	PLSR	100.00%	97.59%	96.67%	92.77%	100.00%	100.00%	90.91%	88.24%	80.61%	89.31%
$EN1_{00}$	PLSR	100.00%	97.59%	86.67%	91.57%	100.00%	100.00%	90.91%	90.59%	78.48%	90.08%
EN_{120}	PLSR	93.33%	92.77%	96.67%	87.95%	100.00%	100.00%	93.94%	91.76%	81.21%	89.31%
ENAll	LS-SVM	100.00%	96.39%	100.00%	96.39%	100.00%	100.00%	93.94%	91.76%	100.00%	96.95%
ENMax	LS-SVM	100.00%	98.80%	100.00%	97.59%	96.67%	100.00%	96.97%	95.29%	99.39%	96.95%
ENMin	LS-SVM	100.00%	98.80%	96.67%	100.00%	100.00%	100.00%	96.97%	96.47%	100.00%	98.47%
EN_{Sum}	LS-SVM	100.00%	100.00%	100.00%	100.00%	96.67%	98.85%	93.94%	92.94%	99.70%	98.47%
ENDiff	LS-SVM	53.33%	83.13%	83.33%	77.11%	70.00%	78.16%	100.00%	81.18%	70.91%	86.26%
EN_{10}	LS-SVM	100.00%	95.18%	100.00%	95.18%	100.00%	95.40%	93.94%	90.59%	100.00%	97.71%
EN_{20}	LS-SVM	100.00%	97.59%	100.00%	91.57%	93.33%	96.55%	90.91%	89.41%	98.79%	96.95%
EN_{40}	LS-SVM	100.00%	97.59%	100.00%	93.98%	90.00%	98.85%	90.91%	92.94%	99.09%	96.95%
EN_{60}	LS-SVM	100.00%	98.80%	96.67%	97.59%	96.67%	100.00%	90.91%	91.76%	99.70%	97.71%
EN_{80}	LS-SVM	100.00%	98.80%	96.67%	98.80%	100.00%	98.85%	93.94%	94.12%	99.70%	96.18%
EN_{100}	LS-SVM	100.00%	100.00%	96.67%	97.59%	100.00%	95.40%	96.97%	91.76%	100.00%	97.71%
EN_{120}	LS-SVM	100.00%	100.00%	100.00%	95.18%	100.00%	96.55%	93.94%	89.41%	100.00%	98.47%

LS-SVM, least squares support vector machine; PLSR, partial least squares regression.

Table 4. Prediction of time after vibrational damage for strawberries with vibration damage

Time	Feature variables	Calibration method	Calibration			Prediction				AB_RMSE
			R_c	Rc^2	RMSEC	R_p	Rp^2	RMSEP	RPD	
all	ENAll	PLSR	0.967	0.936	0.288	0.941	0.882	0.339	2.955	0.051
all	ENMax	PLSR	0.953	0.907	0.346	0.928	0.851	0.382	2.675	0.036
0 h	ENAll	PLSR	0.995	0.990	0.116	0.993	0.983	0.127	8.215	0.011
0 h	EN_{Sum}	PLSR	0.993	0.987	0.132	0.992	0.982	0.131	7.554	0.001
0.5 h	ENAll	PLSR	0.994	0.988	0.125	0.991	0.979	0.137	7.603	0.012
0.5 h	EN_{Sum}	PLSR	0.993	0.986	0.135	0.991	0.977	0.140	7.574	0.005
1 h	ENAll	PLSR	0.990	0.980	0.156	0.990	0.976	0.177	6.411	0.022
1 h	ENMax	PLSR	0.981	0.963	0.212	0.980	0.960	0.226	5.028	0.014
2 h	ENAll	PLSR	0.990	0.979	0.168	0.955	0.904	0.266	3.233	0.098
2 h	ENMax	PLSR	0.983	0.966	0.214	0.972	0.922	0.240	3.591	0.025
all	ENAll	LS-SVM	0.999	0.998	0.055	0.980	0.959	0.201	4.993	0.146
all	ENMax	LS-SVM	0.999	0.997	0.059	0.983	0.967	0.180	5.478	0.121
0 h	ENAll	LS-SVM	1.000	0.999	0.027	0.993	0.985	0.123	8.258	0.096
0 h	ENMax	LS-SVM	1.000	1.000	0.002	0.992	0.983	0.129	7.840	0.127
0.5 h	ENAll	LS-SVM	0.999	0.999	0.039	0.993	0.984	0.119	8.529	0.080
0.5 h	ENMax	LS-SVM	1.000	0.999	0.030	0.993	0.985	0.113	8.368	0.082
1 h	ENAll	LS-SVM	0.998	0.997	0.065	0.991	0.979	0.163	7.412	0.098
1 h	EN_{120}	LS-SVM	1.000	1.000	0.000	0.993	0.986	0.135	8.478	0.135
2 h	ENAll	LS-SVM	1.000	0.999	0.029	0.976	0.951	0.190	4.552	0.161
2 h	ENMax	LS-SVM	1.000	1.000	0.005	0.991	0.981	0.119	7.389	0.114

LS-SVM, least squares support vector machine; PLSR, partial least squares regression; R_c, correlation coefficient of calibration; RMSEC, root-mean-square error of calibration; RMSEP, root-mean-square error of prediction; RPD, residual prediction deviation; R_p, correlation coefficient of prediction. AB_RMSE: the absolute difference between RMSEC and RMSEP.

time after vibrational damage, which was 0 days (right after vibration treatment), 1, 2, and 3 days. For 0, 0.5, 1, and 2 h, 90 samples were used for the calibration and another 30 samples for the prediction. For all four days, 360 samples were used for the calibration and another 120 samples for the prediction. Table 4 shows the results for the best e-nose feature model and ENAll model in each sample set. When the PLSR algorithm was used for model calibration, the fruit without vibration treatment obtained the best results, with an RPD over 7, showing that as the time after harvest increased, the VOCs of the strawberries changed, such that the e-nose could distinguish between different storage times. As the vibration duration increased from 0.5 to 2 h, the prediction accuracy of the models gradually decreased (the RPD decreased from 7.603 and 7.574 to only 3.233 and 3.591). When the samples from all vibration times were considered, the RPD values further decreased to only 2.955 and 2.675. When the LS-SVM algorithm was used for model calibration, the results, similar to those of the models based on samples with less vibration time, obtained better predictions. As the time that the fruit was subjected to vibrations increased, the prediction accuracy of the model gradually decreased. Moreover, the results of the models based on the samples from all vibration times were relatively poorer than those based on the samples from each vibration time. Nevertheless, the results of the LS-SVM models were generally better than those of the PLSR models, especially for the models based on the samples from all vibration times, showing that LS-SVM is more suitable than PLSR for calibrating hybrid samples. Comparing Tables 2 and 4, it can be seen that predicting the time after the occurrence of vibration obtained better results than predicting the level of vibrational damage.

GC–MS analysis

The relative contents of the VOCs obtained by the non-destructive GC-MS measurement at 0, 2, 4, 6, and 8 days under different levels of vibration are shown in Figure 2. The relative content of esters in strawberries after 0.5 h of vibrations was about 60%. As the vibration time increased to 1 and 2 h, the relative content of esters rose to about 90%. There were about 30% alkenes in the strawberries after vibrations for 0.5 h, and their content did not change notably with storage time. No alkenes were detected in the strawberries that were vibrated for 1 and 2 h just after the vibrations (0 days), and the content of alkenes at the other times after vibration was about 5%. In addition, some alcohols were also detected in the strawberries that were subjected to vibration, the content of which was the highest just after the vibrations (0 days), accounting for about 4% and gradually decreasing to about 1% with an increase in storage time.

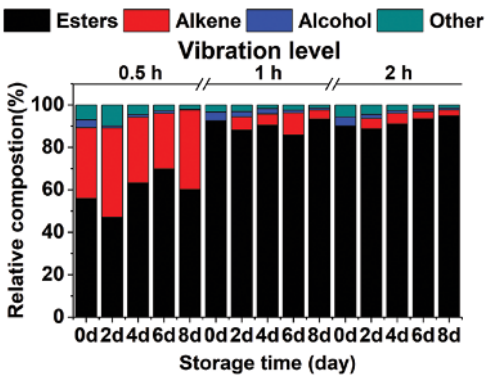

Figure 2. Non-destructive gas chromatography–mass spectrophotometry (GC–MS) detection results for the relative content of volatile substances (VOCs) from strawberries with different vibration levels.

After further analysis of the specific changes in the content of VOCs acquired by the non-destructive GC–MS measurement, it can be seen that after the fruit was mechanically damaged by vibrations, the content of some substances changed (Figure 3). The content of methyl *butanoate* was positively correlated with the level

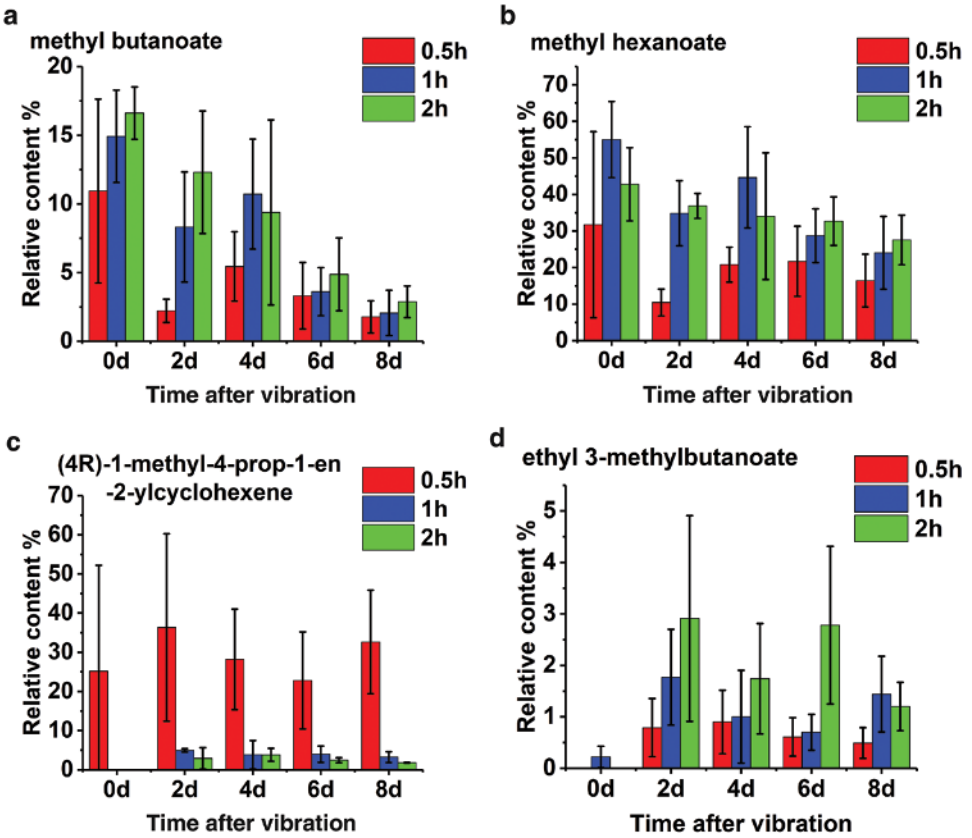

Figure 3. Relative content of some volatile substances (VOCs) of strawberries with different vibration levels measured by the non-destructive gas chromatography–mass spectrophotometry (GC–MS) measurement.

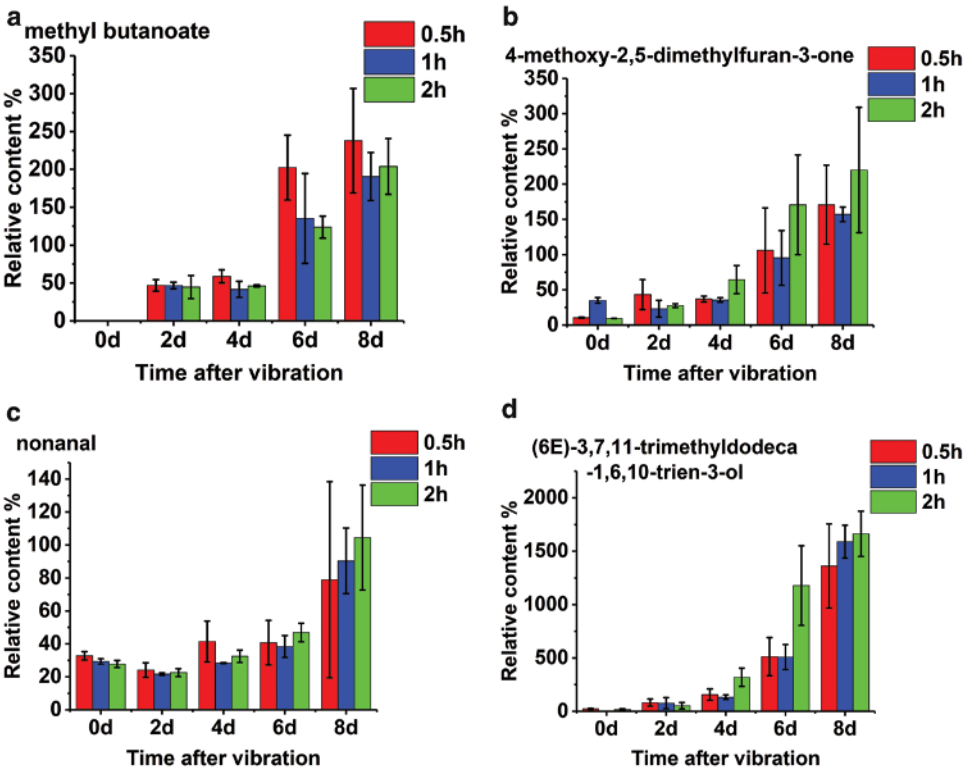

Figure 4. Relative content of some volatile substances (VOCs) of strawberries with different vibration levels measured by the destructive gas chromatography–mass spectrophotometry (GC–MS) measurement.

of vibrations at the early time-points after vibrations. However, this difference was not obvious in the later stages of storage (Figure 3a). The content of methyl hexanoate, during the entire storage period, had a correlation with the level of vibrations (Figure 3b). When the fruit was subjected to severe vibrations (1 and 2 h), the content of (4R)-1-methyl-4-prop-1-en-2-ylcyclohexene was significantly lower than that of the fruit that experienced light vibrations (0.5 h) during the whole storage period (Figure 3c). For ethyl 3-methylbutanoate, there was no difference in content in the fruits treated with different vibration levels at 0 d, but their content was related to the vibration level after two days of storage (Figure 3d).

Figure 4 shows the changes of some VOCs in strawberries obtained by the destructive GC–MS measurement after different mechanical damage treatments during storage. The content of methyl butanoate was low in the early storage period and then increased in the later storage period; however, the increase of content in fruits with more severe vibrational damage was not as high as that in fruits with less damage (Figure 4a). Conversely, the contents *of* 4-methoxy-2,5-dimethylfuran-3-one (Figure 4b), nonanal (Figure 4c), and (6E)-3,7,11-trimethyldodeca-1,6,10-trien-3-ol (Figure 4d) also increased in the late storage period, but the more severe the damage was, the more the contents increased.

Discussion

Previous studies showed that the VOCs of fruit can be affected by many factors, including fruit development and ripening, postharvest treatment, and pathogenic fungal diseases and pests. A study on persimmons by Taiti *et al.* (2018) showed that when the fruits were ripe enough to eat, their concentrations of terpenes, sulfur compounds, lactones, and green leaf volatiles were low, whereas those of short-chain alcohols and aldehydes were relatively high. By using GC-IMS technology to characterize the VOCs of avocado, Liu *et al.* (2020) found that the content of phenol and acrolein gradually decreased and finally disappeared during the ripening process. According to Cai *et al.* (2020), besides enhancing the chilling tolerance of peach, nitric oxide treatment can lead to higher emissions of some VOCs, such as straight-chain esters and lactones, by regulating the synthesis of fatty acids. In another work, exogenous melatonin treatment delayed strawberry deterioration and did not significantly affect the abundance of VOCs, except for two important ones, 2-methylbutanoate and ethyl hexanoate (El-Mogy *et al.*, 2019). Chalupowicz *et al.* (2020) observed that fungal infection changed the VOCs of citrus, especially limonene, and is thus a promising marker for pathogen activity. Gong *et al.* (2019) identified some VOCs released by inoculated apples and found that apples with different susceptibilities showed related VOC changes under pathogen infection. In addition to the above factors, when fruit is mechanically damaged, its VOCs will also change. Thus, researchers are interested in what occurs to the VOCs released by the fruit after suffering mechanical damage. For blueberries, the impact made the fruit more susceptible to fungal infection and caused changes in VOCs, such as increased aldehyde content (Polashock *et al.*, 2007). Our previous research found that when yellow peach fruit suffered compression damage, the relative content of 2(3H)-Furanone, 5-hexyldihydro-, 2H-Pyran-2-one, tetrahydro-6-pentyl, and pentadecane decreased with an increase in the level of compression damage; the relative content of ethyl caproate, ethyl acetate, and ethyl trans-4-decenoate increased with an increase in the level of compression damage, and the relative content of 4-Octenoic acid, methyl ester, (Z) was related to the level of compression damage immediately after the damage (Yang *et al.*, 2020). In the current study, the data from GC–MS indicated that the types and contents of VOCs in strawberries can be affected when the fruit suffers vibrational damage, as well as during storage. These changes allowed e-nose technology to detect strawberries that suffered mechanical damage. Moreover, to study what happens to the VOCs released by the whole fruit rather than the tissue homogenate, this study used a non-destructive method to obtain the GC–MS signal. To monitor the changes of VOCs in the fruit throughout the supply chain, more research is needed based on an analysis of the whole fruit (instead of obtaining a homogenate of the fruit tissue through a destructive method), followed by using GC–MS to analyse the changes of VOCs in the fruits that suffered mechanical damage.

Compared to GC–MS technology, which is often used to separate and determine specific VOCs, e-nose technology mainly analyzes and detects VOCs as a whole. In studies on fruit VOCs, e-nose is often used for species classification, quality prediction and disease and freshness detection. In the area of damage detection, Demir *et al.* (2011) acquired an e-nose signal from blueberries on different days after impact damage and obtained 100% correct classification rates for days 2, 10, 17, and 24. In another study, Ren *et al.* (2018) released apples at different drop heights to simulate various degrees of mechanical damage, and then collected the e-nose data and classified the damaged apples using a back-propagation neural network. In a previous study, we used e-nose technology to detect yellow peaches with compression damage (Yang *et al.*, 2020). The results showed that the RPD values of the best prediction models for damage level and time after damage were 2.139 and 2.114, respectively, and the best CAR for discriminating the damaged fruit was 93.33%. However, the results of this study also showed that good predictive results could be obtained based on the data acquired at only 24 h after the compression damage occurred. When the data were acquired at 4 or 8 h after the compression damage occurred, the predictive results were not good. In the current study, we found that the vibrational damage detection models established at 0, 1, 2, and 3 h after the occurrence of vibrations all obtained good detection results. Moreover, in selecting a metrology modelling algorithm for analysing an e-nose signal, this study found that nonlinear LS-SVM modelling is better than using the linear PLSR algorithm, which is similar to the results of our previous research (Huang *et al.*, 2015; Wei *et al.*, 2018; Yang *et al.*, 2020).

There are still some problems to be solved before e-nose technology can be used for practical applications. First, most studies, including the current study, primarily analyse whether e-nose technology can detect damaged fruit when the fruit suffers a certain type of mechanical damage, such as an impact, vibration, or compression. However, in industrial practice, there are several mechanical forces acting on the fruit at the same time, and the changes in VOCs released by these forces should be studied. Secondly, factors like fruit variety, orchard, cultivation method, and harvest year may have an influence on the changes in VOCs after the fruit is mechanically damaged. Therefore, it is necessary to collect more comprehensive samples for modelling for the model to be used in practice applications. Third, many current studies are based on large desktop e-nose instruments, which are not suitable for use in the fruit supply chain. It is necessary to develop miniaturized and low-cost e-nose instruments that are more suitable for monitoring fruit VOCs in transportation and storage environments. In addition, environmental temperature and humidity can also affect the collection of e-nose signals, so further research is needed in this area.

Conclusions

This study demonstrated the potential of using e-nose technology to rapidly and non-destructively predict the levels of vibrational damage of strawberries, distinguish the damaged fruit, and predict the day after the damage happened. When the samples from all four sampling days were considered for modelling, the LS-SVM-ENSum model obtained the best results for predicting the damage level, with an RPD value of 2.984 and an RMSEP of 0.370. On the other hand, when the models were established based on the samples from one sampling day after vibrations, the results were generally better than those of the all-sample models, but the prediction accuracy of the latter was still satisfactory. Notably, samples contained in the latter model were more similar to an actual situation. The models for discriminating whether the fruit was damaged by vibrations also obtained good detection accuracy. The best LS-SVM model for the total samples from all sampling days provided an average CAR for calibration and prediction of 99.24%, where that of the best PLSR model was 87.61%. The LS-SVM algorithm also obtained the best results, with an RPD value of about 5 when predicting the days after vibration, especially when the total samples were used for modelling. Both the non-destructive and GC–MS measurements show that the content of some VOCs changed after the fruit suffered vibrational damage, including methyl butanoate, methyl hexanoate, (4R)-1-methyl-4-prop-1-en-2-ylcyclohexene, ethyl 3-methylbutanoate, 4-methoxy-2,5-dimethylfuran-3-one, nonanal, and (6E)-3,7,11-trimethyldodeca-1,6,10-trien-3-ol. Although there was not a clear relationship between the change in content and the vibration level or time, these changes were the basis for e-nose technology to detect fruits damaged by vibrations. These findings illustrate the novel promise of using e-nose technology to rapidly and non-destructively detect damaged fruit in the postharvest supply chains.

Authors' Contributions

Conceptualization, Di Wu; Data curation, Yuchen Zhang and Jingshan Rao; Formal analysis, Yuchen Zhang, Jingshan Rao, and Zhichao Yang; Funding acquisition, Chongde Sun, Di Wu, and Shaojia Li; Investigation, Yuchen Zhang and Jingshan Rao; Methodology, Di Wu; Project administration, Di Wu and Kunsong Chen; Resources, Di Wu; Software, Di Wu; Supervision, Di Wu and Kunsong Chen; Validation, Di Wu and Jingshan Rao; Visualization, Jingshan Rao, Yuchen Zhang and Zhichao Yang; Writing—original draft: Jingshan Rao and Zhichao Yang; Writing—review and editing: Di Wu.

Funding

This research was funded by the National Key Research and Development Program of China (2017YFD0401302), Zhejiang Provincial Key Research and Development Program of China (2019C02074), and Talent Project of Zhejiang Association for Science and Technology, China (2018YCGC006).

Conflict of Interest

The authors declare no conflict of interest.

References

Aaby, K., Skrede, G., Wrolstad, R. E. (2005). Phenolic composition and antioxidant activities in flesh and achenes of strawberries (Fragaria ananassa). *Journal of Agricultural and Food Chemistry,* 53(10): 4032–4040.

Cai, H. F., Han, S., Yu, M. L., *et al.* (2020). Exogenous nitric oxide fumigation promoted the emission of volatile organic compounds in peach fruit during shelf life after long-term cold storage. *Food Research International,* 133: 109135.

Centonze, V., Lippolis, V., Cervellieri S., *et al.* (2019). Discrimination of geographical origin of oranges (*Citrus sinensis* L. Osbeck) by mass spectrometry-based electronic nose and characterization of volatile compounds. *Food Chemistry,* 277: 25–30.

Chalupowicz, D., Veltman, B., Droby, S., *et al.* (2020). Evaluating the use of biosensors for monitoring of *Penicillium digitatum* infection in citrus fruit. *Sensors and Actuators B: Chemical*, 311: 127896.

Chen, X. J., Xu, Y. L., Meng, L. Y., *et al.* (2020). Non-parametric partial least squares - discriminant analysis model based on sum of ranking difference algorithm for tea grade identification using electronic tongue data. *Sensors and Actuators B: Chemical*, 311: 127924.

Demir, N., Ferraz, A. C., Sargent, *et al.* (2011). Classification of impacted blueberries during storage using an electronic nose. *Journal of the Science of Food and Agriculture,* 91: 1722–1727.

El-Mogy, M. M., Ludlow, R. A., Roberts, C., *et al.* (2019). Postharvest exogenous melatonin treatment of strawberry reduces postharvest spoilage but affects components of the aroma profile. *Journal of Berry Research*, 9(2): 297–307.

Galvao, R. K. H., Araujo, M. C. U., Jose, G. E., *et al.* (2005). A method for calibration and validation subset partitioning. *Talanta*, 67(4): 736–740.

Giampieri, F., Tulipani, S., Alvarez-Suarez, J. M., *et al.* (2012). The strawberry: composition, nutritional quality, and impact on human health. *Nutrition,* 28(1): 9–19.

Gong, D., Bi, Y., Li, Y. C., *et al.* (2019). Both Penicillium expansum and trichothecim roseum infections promote the ripening of apples and release specific volatile compounds. *Frontiers in Plant Science,* 10: 338.

Hamiltonkemp, T. R., Archbold, D. D., Collins, R. W., *et al.* (2003). Emission patterns of wound volatile compounds following injury of ripe strawberry fruit. *Journal of the Science of Food and Agriculture*, 83(4): 283–288.

Held, M. T., Anthon, G. E., Barrett, D. M. (2015). The effects of bruising and temperature on enzyme activity and textural qualities of tomato juice. *Journal of the Science of Food and Agriculture,* 95(8): 1598–1604.

Huang, L. X., Liu, H. R., Zhang, B., *et al.* (2015). Application of electronic nose with multivariate analysis and sensor selection for botanical origin identification and quality determination of honey. *Food & Bioprocess Technology*, 8(2): 359–370.

Huang, L. X., Meng, L. W., Zhu, N., *et al.* (2017a). A primary study on forecasting the days before decay of peach fruit using near-infrared spectroscopy and electronic nose techniques. *Postharvest Biology and Technology*, 133: 104–112.

Huang, L. X., Zhou, Y. B., Meng, L. W., *et al.* (2017b). Comparison of different CCD detectors and chemometrics for predicting total anthocyanin content and antioxidant activity of mulberry fruit using visible and near infrared hyperspectral imaging technique. *Food Chemistry,* 224: 1–10.

Jaeger, S. R., Antunez, L., Ares, G., *et al.* (2016). Consumers' visual attention to fruit defects and disorders: A case study with apple images. *Postharvest Biology and Technology*, 116: 36–44.

Jetti, R. R., Yang, E., Kurnianta, A., *et al.* (2007). Quantification of selected aroma-active compounds in strawberries by headspace solid-phase microextraction gas chromatography and correlation with sensory descriptive analysis. *Journal of Food Science,* 72(7): S487–S496.

Kader, A. A. (2002). *Postharvest Technology of Horticultural Crops* (3rd ed.). University of California, Agriculture and Natural Resources: Richmond, CA.

Larsen, M., Poll, L. (1992). Odour thresholds of some important aroma compounds in strawberries. *Zeitschrift für Lebensmittel-Untersuchung und Forschung*, 195(2): 120–123.

Li, L., Song, J., Kalt, W., *et al.* (2013). Quantitative proteomic investigation employing stable isotope labeling by peptide dimethylation on proteins of strawberry fruit at different ripening stages. *Journal of Proteomics,* 94: 219–239.

Li, J. Z., Liu, H. X., Yao, X. J., *et al.* (2007). Structure-activity relationship study of oxindole-based inhibitors of cyclin-dependent kinases based on least-squares support vector machines. *Analytica Chimica Acta*, 581(2): 333–342.

Li, Z. G., Thomas, C. (2014). Quantitative evaluation of mechanical damage to fresh fruits. *Trends in Food Science & Technology*, 35(2): 138–150.

Li, Z. G., Yang, H. L., Li, P. P., *et al.* (2013). Fruit biomechanics based on anatomy: a review. *International Agrophysics*, 27(1): 97–106.

Liu, Y. J., Bu, M. T., Gong, X., *et al.* (2020) Characterization of the volatile organic compounds produced from avocado during ripening by gas chromatography ion mobility spectrometry. *Journal of the Science of Food and Agriculture*, in press.

Liu, Q., Zhao, N., Zhou, D. D., *et al.* (2018). Discrimination and growth tracking of fungi contamination in peaches using electronic nose. *Food Chemistry*, 262: 226–234.

Liu, C. H., Zheng, H. H., Sheng, K. L., *et al.* (2018). Effects of melatonin treatment on the postharvest quality of strawberry fruit. *Postharvest Biology and Technology*, 139: 47–55.

Nguyen, V. T., Nguyen, D. H. H., Nguyen, H. V. H. (2020). Combination effects of calcium chloride and nano-chitosan on the postharvest quality of strawberry (*Fragaria* × *ananassa* Duch.). *Postharvest Biology and Technology*, 162: 111103.

Pan, L. Q., Zhang, W., Zhu, N., *et al.* (2014). Early detection and classification of pathogenic fungal disease in post-harvest strawberry fruit by electronic nose and gas chromatography–mass spectrometry. *Food Research International*, 62: 162–168.

Parrapalma, C., Ubeda, C., Gil, M., *et al.* (2019). Comparative study of the volatile organic compounds of four strawberry cultivars and it relation to alcohol acyltransferase enzymatic activity. *Scientia Horticulturae*, 251: 65–72.

Polashock, J. J., Saftner, R. A., Kramer, M. (2007). Postharvest highbush blueberry fruit antimicrobial volatile profiles in relation to anthracnose fruit rot resistance. *Journal of the American Society for Horticultural Science*, 132(6): 859–868.

Prat, L., Espinoza, M. I., Agosin, E., *et al.* (2014). Identification of volatile compounds associated with the aroma of white strawberries (*Fragaria chiloensis*). *Journal of the Science of Food and Agriculture,* 94: 752–759.

Ren, Y. M., Ramaswamy, H. S., Li, Y., *et al.* (2018). Classification of impact injury of apples using electronic nose coupled with multivariate statistical analyses. *Journal of Food Process Engineering*, 41(5): e12698.

Srivastava, S., Sadistap, S. (2018). Data processing approaches and strategies for non-destructive fruits quality inspection and authentication: a review. *Journal of Food Measurement and Characterization*, 12(4): 2758–2794.

Taiti, C., Mancuso, S., Petrucci, W. A., *et al.* (2018). Volatile compound fingerprinting of'Kaki Tipo'and'Rojo Brillante'persimmon fruits at ripe-stage eating quality. *ISHS Acta Horticulturae 1195: VI International Symposium on Persimmon*. 16 October 2016, Valencia, Spain, ISHS, pp. 257–262.

Wei, X., Zhang, Y. C., Wu, D., *et al.* (2018). Rapid and non-destructive detection of decay in peach fruit at the cold environment using a self-developed handheld electronic-nose system. *Food Analytical Methods*, 11(11): 2290–3004.

Wu, D., Sun, D. W. (2013a). Advanced applications of hyperspectral imaging technology for food quality and safety analysis and assessment: A review – Part I: Fundamentals. *Innovative Food Science and Emerging Technologies*, 19: 1–14.

Wu, D., Sun, D. W. (2013b). Advanced applications of hyperspectral imaging technology for food quality and safety analysis and assessment: A review – Part II: Applications. *Innovative Food Science and Emerging Technologies*, 19: 15–28.

Wu, D., Sun, D. W. (2013c). Colour measurements by computer vision for food quality control – A Review. *Trends in Food Science & Technology*, 29(1): 5–20.

Xin, R., Liu, X. H., Wei, C. Y., *et al.* (2018). E-nose and GC-MS reveal a difference in the volatile profiles of white-and red-fleshed peach fruit. *Sensors*, 18(3): 765.

Xing, M. K., Sun, K., Liu, Q., *et al.* (2018). Development of novel electronic nose applied for strawberry freshness detection during storage. *International Journal of Food Engineering*, 14(7–8): 20180111.

Yang, X. Z., Chen, J. H., Jia, L. W., *et al.* (2020). Rapid and non-destructive detection of compression damage of yellow peach using an electronic nose and chemometrics. *Sensors*, 20(7): 1866.

Zabetakis, I., Holden, M. A. (1997). Strawberry flavour: analysis and biosynthesis. *Journal of the Science of Food and Agriculture*, 74(4): 421–434.